Electron escape depth, surface composition, and charge transfer in tetrathiafulvalene tetracyanoquinodimethane (TTF-TCNQ) and related compounds: Photoemission studies

S. F. Lin and W. E. Spicer
Stanford Electronics Laboratories, Stanford University, Stanford, California 94305

B. H. Schechtman
IBM Research Laboratory, San Jose, California 95193

(Received 12 March 1975)

Ultraviolet photoemission spectroscopy (UPS) has been used to study *in-situ*-prepared tetracyanoquinodimethane (TCNQ), $Cs_2(TCNQ)_3$, and tetrathiafulvalene-TCNQ (TTF-TCNQ) thin films. The measurments on $Cs_2(TCNQ)_3$ were made during the charge-transfer reaction between Cs vapor and TCNQ solid, which allows an unambiguous determination of the energy levels near E_F of the $TCNQ^-$ anion. Our results demonstrate that the excess charge of $TCNQ^-$ is localized to a molecular scale and that the TCNQ molecule in solids will normally exist in either the neutral or -1 charge state, and not in a state of shared fractional charge. Quantitative comparison of the UPS spectra between $Cs_2(TCNQ)_3$ and TTF-TCNQ permits a rather complete assignment of the structure in the TTF-TCNQ data. The structures near -1 and -2 eV are assigned to $TCNQ^-$, those near -3 eV to TTF^+ and those near -4 eV to both $TCNQ^0$ and $TCNQ^-$. In addition, the data suggest the presence of TTF^+ states immediately below E_F. From studies of ultrathin films, the electron escape depth is estimated to be less than 10Å in these solids, which indicates a strong representation of the surface electronic structure in our data. TTF-TCNQ deposited at 77°K is found to undergo irreversible changes in both its UPS spectra and its bulk thermal properties upon annealing to room temperature. A model is presented which accounts for these changes in terms of molecular rearrangements upon annealing which are accompanied by altered surface composition of the films and increased ionization of the TTF-TCNQ complex. In room-temperature TTF-TCNQ there is evidence for significant charge transfer, for the presence of some $TCNQ^0$ at the surface, and evidence against any significant surface concentration of TTF^0. In view of this work we suggest (i) that prior uv-photoemission work may have sampled principally the surface and (ii) that the surface of room-temperature TTF-TCNQ films may have a different composition from the bulk.

I. INTRODUCTION

The quasi-one-dimensional, highly conducting organic charge transfer salt tetrathiafulvalene-tetracyanoquinodimethane (TTF-TCNQ) has been subjected to intensive studies recently.[1-11] Among these studies Grobman *et al.*[10] and Nielsen *et al.*[11] have employed photoemission techniques on sublimed samples to gain insight into the electronic properties of this material. Important conclusions on the properties of TTF-TCNQ drawn from these two photoemission studies are the following: (i) Electronic states near the Fermi energy (E_F) are of localized nature, at least on the time scale of the optical excitation process.[10,11] (ii) There is considerable but somewhat less than one ($\sim\frac{2}{3}$) electron transferred from each TTF molecule to a TCNQ molecule,[10] i.e., the ionization of TTF-TCNQ pairs is fractional. (iii) uv photoemission (up to 21.2 eV) probes mainly the bulk electronic structure of TTF-TCNQ; thus the conclusions (i) and (ii) above are valid for the TTF-TCNQ bulk solid and are not strongly influenced by the surface.[10]

In an effort to determine the extent to which the surface electronic structure has been significant in the photoemission experiments, we have measured ultraviolet photoemission spectra (UPS) from TTF-TCNQ films of known thickness to estimate the electron escape depth of this material. The results presented below indicate rather short electron escape depths for this class of materials, and suggest that the UPS spectra are primarily representative of the surface region, in contradiction with earlier conclusions. This result emphasizes that for these materials the surface condition of the sample can be an important factor influencing the reliability of the data. Since a comparison between UPS spectra of TTF-TCNQ and alkali-TCNQ compounds is of great value in sorting out the contributions to the TTF-TCNQ spectra from the various ionic and neutral molecular species,[10,11] it is desirable to perform the aklali-TCNQ experiment under as well-defined surface conditions as possible. Previous studies[10,11] of these systems were not carried out on *in-situ*-prepared samples. In the present work, we report a technique which allowed the investigation of the compound $Cs_2(TCNQ)_3$ with *in-situ* preparation and also allowed us to monitor the charge transfer process by which neutral TCNQ molecules ($TCNQ^0$) are converted into the anion $TCNQ^-$.

Through the comparison of the absolute emission intensities of UPS spectra between TTF-TCNQ and $Cs_2(TCNQ)_3$, and through the observation of the conversion of $TCNQ^0$ into $TCNQ^-$, we were able to determine the origins of different structures in the UPS spectra of TTF-TCNQ. Quasi-dynamic observation of the solid-state reaction $TCNQ^0 \rightarrow TCNQ^-$ using photoemission at intermediate stages during the reaction also furnishes insight into the nature of the charge transfer process in TCNQ-based compounds.

An additional new result of the present studies is the observation of an extreme sensitivity of UPS spectra of TTF-TCNQ films to the substrate temperature at deposition and to the film's subsequent thermal history, which may be related to different surface compositions of the films at different stages of the thermal history. The temperature effects reported here also suggest that sublimed TTF-TCNQ can be prepared in low-temperature states (probably disordered) with quite different electronic properties from the normal state. This behavior is unusual for a molecular solid, and it is probably associated with the long-range nature of the bonding forces in TTF-TCNQ due to the ionic character of the molecular lattice.

II. EXPERIMENTAL METHODS

Energy distribution curves (EDC's) of photoemitted electrons were obtained from threshold energies to 11.8 eV using the ac-modulated retarding potential method[12] and an apparatus described previously.[13] Absolute quantum yields were measured against a calibrated Cs_3Sb photocathode. The ac voltage of the electron energy analyzer was kept below 0.3 eV peak to peak, and the monochromator slits were adjusted to provide an overall energy resolution of better than 0.3 eV. All structures observed in the EDC's had full widths at half-maximum of at least 0.6 eV, which was not limited by the experimental instrumentation. Organic starting materials were purified by repeated recrystallization from acetonitrile in the case of TTF-TCNQ and by both recrystallization and vacuum sublimation in the case of TCNQ. Thin films of TTF-TCNQ or TCNQ were sublimed from a quartz crucible onto polished substrates of Pt or Au-coated Mo, which were heat cleaned at 475 °C in the ultrahigh vacuum just prior to sample deposition. Crucible temperatures were maintained between 110 and 160 °C during deposition of TCNQ and TTF-TCNQ. Base pressure before sublimation was 1×10^{-8} Torr or lower, limited primarily by lack of baking of the vacuum chamber to avoid vaporization and possible decomposition of the organic source materials. During sublimation, pressure increases to typically $(5-7)\times10^{-8}$ Torr were observed. Data recording began within 5–10 min after completion of sample deposition, and the data showed no time-dependent changes except for ultrathin (~10 Å) TTF-TCNQ films deposited onto 77 °K substrates. At room temperature these films resublimed sufficiently rapidly that the characteristic TTF-TCNQ emission disappeared and photoemission characteristic of the metallic substrate reappeared. The substrate temperatures were controlled and could be set continuously between room temperature (RT) and liquid-nitrogen temperature (LNT), and films deposited and held at various substrate temperatures were studied. Approximately ten films each of TCNQ and TTF-TCNQ were prepared and studied, the essential features of the data being well reproduced for both cases.

The chemical and structural properties of vacuum-sublimed TTF-TCNQ films of various thicknesses have been fully characterized and reported elsewhere.[14] It has been established that the sublimed films reproduced bulk properties of single-crystal TTF-TCNQ in all respects except that the electrical conductivity is influenced by polycrystalline grain boundaries.

Thickness of TTF-TCNQ films were measured during deposition using a gold-coated quartz microbalance[15] positioned adjacent to the substrate. The Au coating was employed to simulate the same sticking conditions on the microbalance as for the sample substrate. In the case of depositing onto an LNT substrate, the microbalance measures a lower limit to the sample thickness due to the temperature-dependent difference in sticking probability between sample substrate (LNT) and microbalance (RT). This was corrected for by calibrating the thickness of thick LNT deposited TTF-TCNQ films ($\gtrsim$ 5000 Å) with two other methods.[16] A mechanical measurement using a Gould 200 microtopographer gave 1.3 as the multiplying factor to the microbalance value to obtain the true LNT sample thickness, while optical thickness measurements with a Linnick System Interferometer gave a correction factor of 1.8. In determining the thickness of ultrathin TTF-TCNQ films deposited onto LNT substrates, the conservative value of 1.8 was applied to correct the microbalance result. In the case of TCNQ films deposited onto LNT substrates, this independent calibration was not done and 1.8 was adopted as a reasonable correction factor.

$Cs_2(TCNQ)_3$ was formed by generating Cs vapor from a Joule-heated Cs-chromate channel in the presence of an *in-situ*-deposited TCNQ film. Two stoichiometries have been reported for Cs-TCNQ. The most common one is $Cs_2(TCNQ)_3$ for which

the one $TCNQ^0$ and two $TCNQ^-$ formally associated with two Cs^+ ions are distinguishable in x-ray diffraction.[17] Solution-grown Cs-TCNQ is always $Cs_2(TCNQ)_3$, but upon heating in vacuum this compound loses $TCNQ^0$ and converts to the 1:1 salt Cs(TCNQ).[18] It has been recently established[19] that exposure of Cs solid to TCNQ vapor forms $Cs_2(TCNQ)_3$. In our case TCNQ solid was exposed to Cs vapor. Since the TCNQ molecules were in excess it is quite likely that this reaction also favors the formation of $Cs_2(TCNQ)_3$ over Cs (TCNQ). Support for this is found in electron diffraction studies of the product of a reaction much the same as ours, but on alkali halide substrates.[20]

Low-temperature (LNT to RT) differential thermal analysis (DTA) was performed with a Du Pont 900 thermal analyzer on TTF-TCNQ vacuum deposited onto an LNT sample holder in a separate chamber and subsequently transferred into the analyzer held at LNT. During the transfer there were about 3 sec of exposure time to the ambient air.

III. RESULTS AND DISCUSSION

A. Estimate of electron escape depth

The depth sampled in a photoemission experiment is determined by the electron escape depth.[21] Knowledge of this depth is important for interpretation of photoelectron spectra when there is the possibility of changes in composition from the surfaces to the bulk and/or when there is reason to believe that the electronic properties of the sample may be different in the surface and bulk environments.

In practice, if the optical absorption coefficient α is known, the average escape depth $\bar{L}$ can be estimated through measurement of quantum yields and the use of the equation[22]

$$Y \cong \bar{P}\alpha\bar{L}/(1+\alpha\bar{L}), \tag{1}$$

where $\bar{P} \equiv c_0\bar{p}$, c_0 is the fraction of hot electrons with energy higher than the vacuum level (which can be estimated from optical properties), and $\bar{p}$ is the escape function, i.e., the probability that an electron, once it reaches the surface, will pass out of the solid into the vacuum. The quantity $\bar{p}$ is the escape function averaged over all electrons with kinetic energy higher than the surface potential barrier. The expression in Eq. (1) must be modified in cases where electron scattering significantly adds electrons to the photoemitted current; however, such contributions do not appear to be large in the present studies.

Unfortunately, the optical properties of TTF-TCNQ, TCNQ, or $Cs_2(TCNQ)_3$ are not known in the energy range above about 5 eV. In order to overcome this difficulty, we measured quantum yields and EDC's from films of different thicknesses ranging from greater than 1800 Å to less than 13 Å. From analysis of these data, both α and $\bar{L}$ can be estimated.

In Fig. 1 we present the EDC's for $\hbar\omega = 10.2$ eV from the gold substrate together with those from two TTF-TCNQ films of thicknesses 10–13 and 1800 Å, respectively. Both films were deposited onto a gold substrate kept at liquid-nitrogen temperature. The EDC's from the two TTF-TCNQ films are effectively identical and are quite different from that of gold. This was found to be the case for EDC's taken at many photon energies up to 11.8 eV. This result suggests that the photoemitted electrons originate almost entirely from a region within about 13 Å from the sample-vacuum interface. The same conclusion is borne out by Fig. 2 in which we present the absolute quantum yields of the two films for $\hbar\omega = 5.5$–11.8 eV. We see that the yields for the two films are the same within experimental error (±10%) over the entire spectral range.

To first approximation, the quantum yield for a film of thickness T in this case can be expressed[22,23]

$$Y \cong \int_0^T \bar{P}\alpha e^{-\alpha x} e^{-x/\bar{L}}\, dx$$

$$= \bar{P}\frac{\alpha\bar{L}}{1+\alpha\bar{L}}\left(1 - e^{-(\alpha+1/\bar{L})T}\right), \tag{2}$$

where Y, $\bar{P}$, α, $\bar{L}$ are all functions of photon energy $\hbar\omega$ and x is the distance into the sample from the surface. The fact that the measured quantum yields are independent of sample thickness imposes the condition

$$e^{-(\alpha+1/\bar{L})T} < 0.1 \tag{3}$$

on Eq. (2), even for $T = 13$ Å. Making use of relation (3), Eq. (2), and the experimental value of quantum yield, we can set limits on α and $\bar{L}$.

Based on Eq. (3) we rewrite Eq. (2)

$$Y \cong \bar{P}\alpha\bar{L}/(1+\alpha\bar{L}). \tag{4}$$

Combining Eqs. (3) and (4) and setting $T = 13$ Å we obtain

$$\alpha > 0.077(Y/\bar{P})\ln(1/0.1), \tag{5}$$

$$\bar{L} < 13\frac{\bar{P}}{\bar{P}-Y}\frac{1}{\ln(1/0.1)}, \tag{6}$$

where α is in units of $Å^{-1}$ and $\bar{L}$ in units of Å.

An approximation for $\bar{P}$ must be made. The upper limit on $\bar{P}$ is unity which gives the smallest

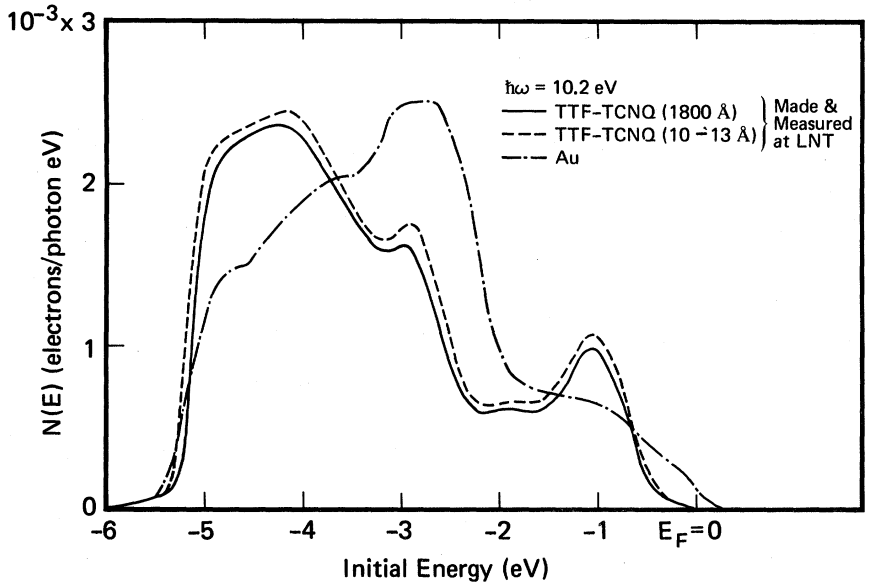

FIG. 1. Comparison of EDC's from heat-cleaned gold and from two LNT-made-and measured TTF-TCNQ films of different thickness. Electron distributions are plotted vs the initial energy of photoelectrons, measured with the Fermi energy E_F as zero.

possible value for $\bar{L}$. The lower limit is set by $\bar{P}=Y$, which from Eq. (5) gives $\alpha > 1.77\times10^{7}$ cm^{-1}, a higher than physically reasonable value for the optical-absorption coefficient.[24] A typical value of $\bar{P}$ is 0.1; however, to be conservative, let us assume $\bar{P}=0.02$ and use the experimental value $Y=6.4\times10^{-3}$ electrons/photon for $\hbar\omega=10.2$ eV, one then obtains $\bar{L}<8.3$ Å and $\alpha>5.7\times10^{6}$ cm^{-1}. If $\bar{P}=0.1$ is taken, one obtains $\bar{L}<6.0$ Å and $\alpha>1.1\times10^{6}$ cm^{-1}. Any larger value taken for $\bar{P}$ further reduces the resulting estimate for $\bar{L}$. In normal practice, a fairly accurate estimate of $\bar{L}$ can be obtained by monitoring the attenuation of electrons originating from the underlying substrate as they pass through known thicknesses of the sample.[25] This technique was not useful in the present work because even the thinnest deposited films allowed no transmission of photoelectrons from the Au substrate to the vacuum. Our above estimates of $\bar{L}$ may therefore be considered somewhat crude. However, there appears to be no way to explain the experimental results for $\hbar\omega=10.2$ eV in a physically consistent manner without taking $\bar{L}\lesssim10$ Å. Similar analyses for $\hbar\omega=8.9$ and 11.6 eV give the same conclusion.

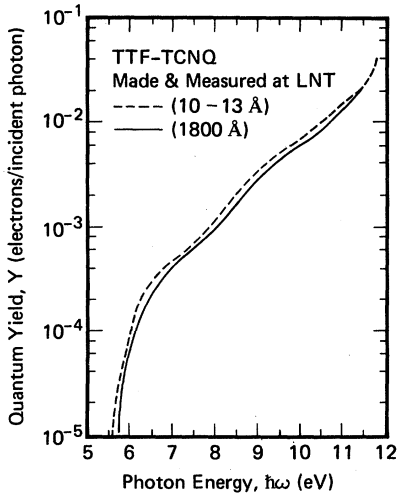

FIG. 2. Spectral distributions of quantum yield of the two LNT-made-and-measured TTF-TCNQ films of Fig. 1.

In Figs. 3 and 4 we show the quantum yields and EDC's of two TCNQ films of thickness 10–13 and 200 Å. Again there is no significant difference of EDC's or yields for two films of different thickness. The electron escape depth in TCNQ is therefore at least as small as in TTF-TCNQ, estimated to be less than 10 Å.

A cautionary note is in order here since the EDC's and yields in Figs. 1 and 2 were from TTF-TCNQ films deposited onto a gold substrate kept at LNT. The short escape depth for TTF-TCNQ is, strictly speaking, derived only the LNT films. As will be seen in the following discussions, the EDC's from these films go through substantial changes as the temperature is increased. Efforts have been made to condense ultrathin TTF-TCNQ films onto a substrate at RT or to retain the ultrathin LNT film at temperatures near RT. Neither has been successful owing to the vapor pressure of TTF-TCNQ ($\sim2\times10^{-10}$ Torr at RT),[26] which causes sublimation of the ultrathin films during times comparable to the measurement time. However, judging from the similar shapes and comparable magnitudes of quantum yields from TTF-TCNQ

films at RT and LNT and also their similarity with $Cs_2(TCNQ)_3$ and TCNQ (ultrathin TCNQ films have been successfully retained at RT) in the region where $\hbar\omega$ > threshold (Fig. 5), the short photoelectron escape depth seems to be characteristic of several TCNQ-based compounds and is probably not a sensitive function of temperature. We conclude then that the escape depth of an RT TTF-TCNQ film is not very different from that of an LNT film.

Considering the crystal structures of TCNQ, $Cs_2(TCNQ)_3$, and TTF-TCNQ (all monoclinic, with $3 < a, b, c < 22$ Å),[17,27,28] this short escape depth implies that the UPS spectra represent only the first few molecular layers. The EDC's and yields must therefore be interpreted with this in mind, as will be evident in Sec. III D. It has been recently reported[14] that on sapphire or quartz substrates, sublimed TTF-TCNQ tends to form films with the crystal *ab* plane parallel to the substrate plane. A similar result has been reported with the cleaved (100) face of NaCl as substrate.[29] Since the *c*-direction molecular spacing is roughly 9 Å, a 10-Å-thick film of TTF-TCNQ would constitute somewhat less than two molecular layers if it retains the bulk molecular stacking and orientation at the surface.

Shorter than usual electron escape depths (< 5 Å) at low kinetic energies (< 10 eV) have been found in certain metals.[21] These metals (Cs, Sr, Ba, Yb and K, etc.) are generally those with low Fermi energies and plasmon energies. Through a Drude analysis, the plasmon energy of TTF-TCNQ has been estimated to be about 1.5 eV,[4] and from thermoelectric power data, the Fermi energy has been estimated to be ~0.14 eV.[30] Each of these values is less than the corresponding value for the above metals, e.g., for Cs $E_P = 3.0$ eV and $E_F = 1.5$ eV,[31] and hence the apparent correlation between small Fermi and plasmon energies and short escape depths may carry over into organic solids, for which little data are available.

At present we do not have a microscopic understanding of the short escape depth for TTF-TCNQ.

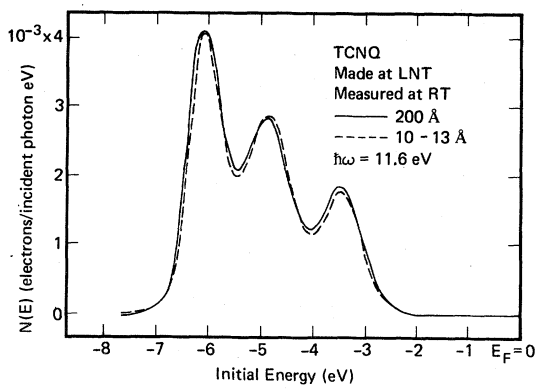

FIG. 4. Normalized EDC's for $\hbar\omega = 11.6$ eV from the two TCNQ films of Fig. 3.

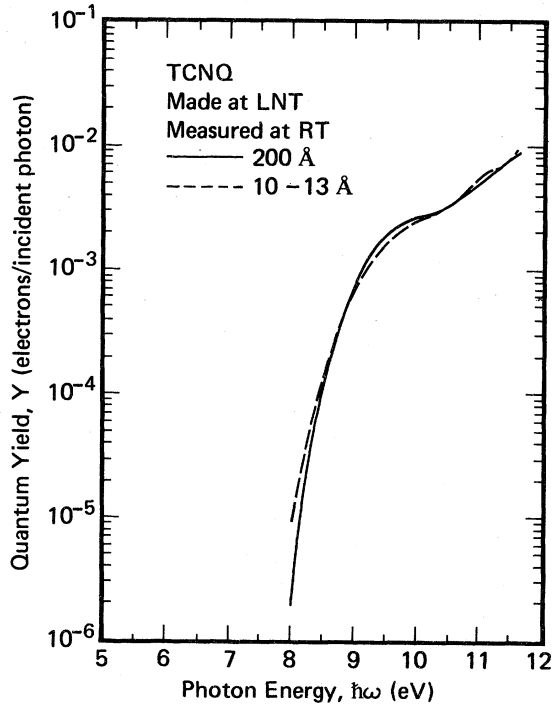

FIG. 3. Spectral distributions of quantum yield of two TCNQ films of different thickness.

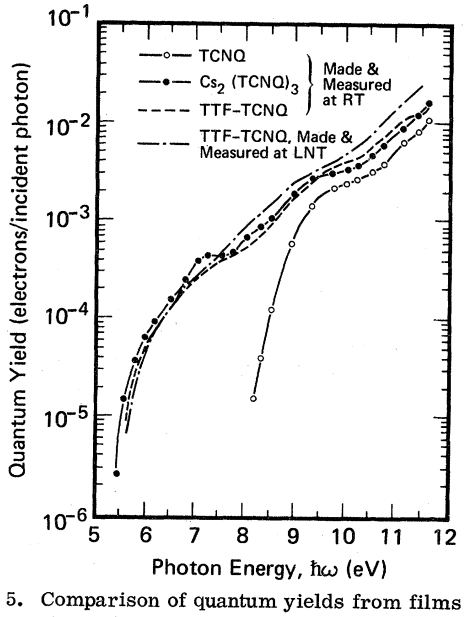

FIG. 5. Comparison of quantum yields from films of TCNQ, $Cs_2(TCNQ)_3$, RT-made-and-measured TTF-TCNQ, and LNT-made-and-measured TTF-TCNQ.

Several factors may be involved. In organic solids, the final-state wave functions a few eV above the vacuum level are perhaps less extended than for inorganic solids. Therefore the photoelectron group velocity and hence its mean free path would be correspondingly smaller. In the only other direct measurement of the escape depth for an organic solid of which we are aware,[32] it was found that $\bar{L} = 11$ Å in phthalocyanine for $\hbar\omega = 7.8$ eV, i.e., for average electron kinetic energies of only about 1 eV.

B. Conversion of $TCNQ^0$ to $TCNQ^-$

As indicated in the introduction, an issue of importance in understanding TTF-TCNQ is the question of how much charge is transferred from TTF to TCNQ. In order to address this question with photoemission techniques, it is first necessary to clearly establish the energy-level structure in the vicinity of the Fermi energy for both $TCNQ^0$ and $TCNQ^-$. A novel approach[33] to determine this information was undertaken here. UPS experiments were used to monitor the changes in the electronic structure of $TCNQ^0$ as it was converted to $TCNQ^-$ during the reaction between TCNQ solid and Cs vapor. We believe this to be the first investigation of the energy-level structure of an organic donor-acceptor solid conducted during the bulk charge transfer reaction between the components. These experiments not only enabled us to obtain a clear picture of the energy levels of $TCNQ^-$, but also provided the first photoemission studies of an alkali-TCNQ complex prepared *in situ*. By controlling the amount of Cs exposure during the reaction, the conversion process of $TCNQ^0 \rightarrow TCNQ^-$ can be observed at intermediate stages.

Figures 6 (a) and 6 (b) show the UPS spectra at $\hbar\omega = 8.5$ and 10.2 eV, respectively, at three different stages of the reaction between a TCNQ film and cesium vapor. The Fermi energy indicated in the figure was determined by photoemission from the substrate and verified by photoemission from a copper shutter at the rear of the collector can. Before cesiation, there is negligible electron population between E_F and -2.5 eV in Fig. 6. The -3.5-eV peak corresponds to the highest-lying π orbital of $TCNQ^0$. As the vapor-solid reaction takes place and the $TCNQ^0 \rightarrow TCNQ^-$ conversion proceeds, two weak peaks (at -1.0 and -2.1 eV) begin to appear in the previously unpopulated region. When the reaction reaches completion and a stable, saturated condition is attained, these two peaks have developed to the point where they dominate the spectra above -2.5 eV.

Three important points can be made about Fig. 6. First, the positions and the intensity ratio of the two new peaks remain constant during the entire cesiation process, which underscores the localized nature of the orbitals involved in accepting the transferred electrons. It can also be deduced from this result that in this system the TCNQ species exist as either $TCNQ^0$ or $TCNQ^-$, and never with some intermediate level of ionization. The second point to note is that the intensity ratio of the two new peaks remains approximately 1 to 2 throughout the reaction, which is consistent with the interpretation that the -1.0-eV peak corresponds to the singly-occupied highest π orbital of $TCNQ^-$, while the -2.1-eV peak arises from the doubly-occupied second-highest π orbital of $TCNQ^-$. According to several recent electronic structure calculations for TCNQ,[34-37] these orbitals are of b_{2g} and b_{1u} symmetry, respectively. The UPS spectra of $TCNQ^0$ (dash-dot curves in Fig. 6 and Refs. 10 and 11) indicate that in the neutral molecule the highest-occupied (b_{1u}) level is at least 3 eV below the lowest-empty (b_{2g}) level. Our assignment of the -1.0-eV peak in the photoemission from $Cs_2(TCNQ)_3$ to the b_{2g} affinity level therefore indicates that upon occupation by an electron this

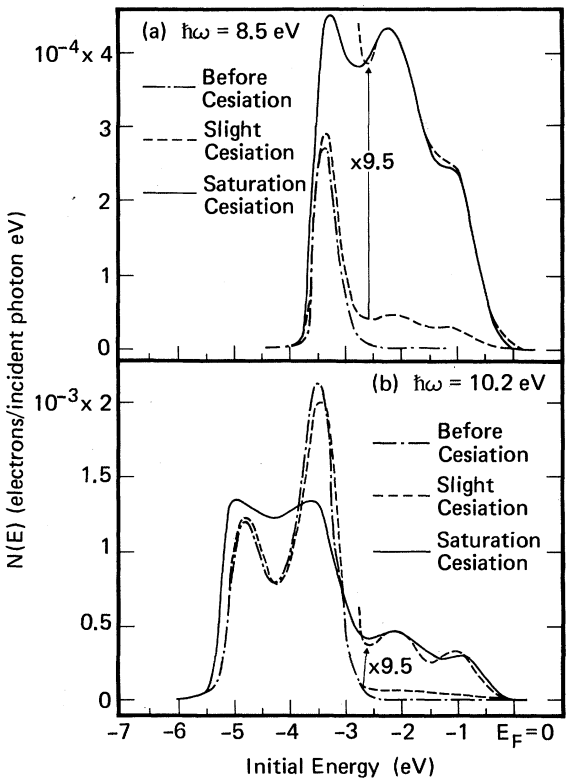

FIG. 6. EDC's of Cs-TCNQ system at (a) $\hbar\omega = 8.5$ eV and (b) $\hbar\omega = 10.2$ eV. Dash-dot line shows $TCNQ^0$ spectra, broken line spectra after 3 min of cesium exposure and solid line after 25 min of cesium exposure, both at an average Cs pressure of $\sim 5 \times 10^{-8}$ Torr.

orbital moves down in energy by at least 1 eV. The -2.1-eV peak, attributed to the b_{1u} level, moves up from its location at -3.5 eV upon anion formation. Thus the separation between the lowest-empty and highest-occupied levels in $TCNQ^0$ has been reduced by more than 2 eV upon conversion to $TCNQ^-$.

This large change in orbital separation upon ionization may be understood from the following considerations: $TCNQ^0$ is a strong electron acceptor with a molecular electron affinity of 2.8 eV.[38] When an electron is added to this system, the TCNQ orbitals relax to lower the total energy of the anion. This relaxation takes the form of a downward shift of the newly occupied orbital, accompanied by varying degrees of upward shifts of the lower-lying occupied orbitals. The large magnitude of the orbital readjustments in $TCNQ^-$ is another manifestation of the high degree of localization of the excess electronic charge on a molecular scale. Figure 7 shows a schematic diagram of the orbital level shifting. Also shown in the figure are comparisons of level spacings in $TCNQ^0$ and $TCNQ^-$ from our experimental results and the theoretical results of very recent extended-Hückel,[34] multiple-scattering $X\alpha$,[35] and *ab initio*[36] calculations. For the latter two calculations, the numbers given are for the weighted averages of singlet and triplet transition energies where appropriate. It is interesting that the simplest of the three calculations, the extended Hückel, seems to give the best results for the b_{2g}-to-b_{1u} level spacing in $TCNQ^-$.

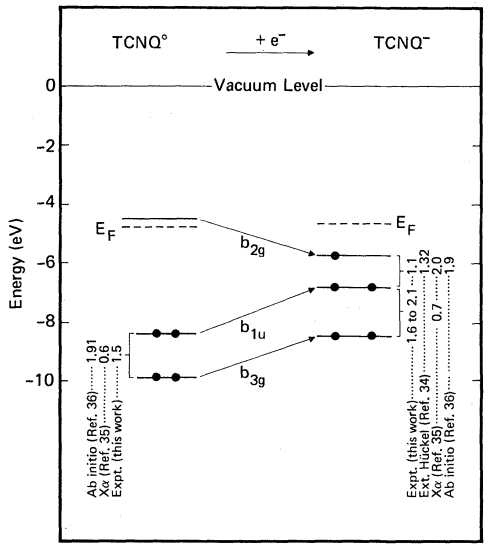

FIG. 7. Schematic diagram of orbital rearrangement in TCNQ due to electron addition and comparison of level spacings with recent calculations.

Finally, the -3.5-eV peak of $TCNQ^0$ in Fig. 6 (b) decreased in intensity by about $\frac{1}{3}$ and moved to -3.7 eV upon cesiation. In view of the 2:1 stoichiometry of $TCNQ^-$ to $TCNQ^0$ in $Cs_2(TCNQ)_3$,[17] we would expect the strength of the $TCNQ^0$ peak to decrease by $\frac{2}{3}$. However, it is possible that the matrix elements for transitions from these states were altered owing to changes in the final-state wave functions upon complex formation. It is also likely that in this energy range there are $TCNQ^-$ states that contribute part of the emission intensity, since $TCNQ^0$ has high density of occupied states below -3.5 eV (see Fig. 4), and some of these states are expected to shift upward upon ionization. Evidence for this occurs in data reported for $K^+(TCNQ)^-$ at $\hbar\omega = 21.2$ eV,[10] which show a shoulder at -4.2 eV in the UPS spectra. It is probable that the combination of $TCNQ^-$ states near -4.2 eV and $TCNQ^0$ states at -3.5 eV results in the -3.7-eV peak in $Cs_2(TCNQ)_3$ and in the greater intensity of this peak compared to the intensity expected if it were derived from a single orbital of $TCNQ^0$.

C. Comparison of TTF-TCNQ and Cs_2 $(TCNQ)_3$

In Fig. 8 we compare the UPS spectrum of TTF-TCNQ to that of $Cs_2(TCNQ)_3$. The similarity between the two is evident. The emission intensity above -2 eV in TTF-TCNQ appears to arise predominantly from $TCNQ^-$ as we compare the spectra in Figs. 8 (a) and 8 (b). This is in agreement with the contention that there is considerable charge transfer from TTF to TCNQ. Also by comparison of Figs. 8 (a) and 8 (b), the -3.6-eV peak in TTF-TCNQ appears to come jointly from $TCNQ^0$ and $TCNQ^-$, as in the case of the -3.7-eV peak in $Cs_2(TCNQ)_3$. Thus our spectra contain evidence, at least at the sample surface, for the presence of $TCNQ^0$ in TTF-TCNQ, consistent with earlier interpretations based on both UPS and XPS (x-ray photoemission) data.[10]

The subtle distinctions between Figs. 8 (a) and 8 (b) are better illustrated in the difference curve of Fig. 8 (c), which was obtained by direct subtraction of the absolute energy distributions per incident photon. In Fig. 8 (c), E_F was chosen as a common energy reference for the two materials (almost identical results obtain by choosing the vacuum level as a reference), and the numerical error in the ordinate values arising from the subtraction process is estimated to be 10%. Since Cs^+ does not contribute to the valence states of $Cs_2(TCNQ)_3$, structures in Fig. 8 (c) are attributed to emissions from TTF. The extra emission near E_F centered around -0.5 eV most likely arises from the singly-occupied b_{1u} π level of

TTF^+,[34,35] which is buried under the highest-occupied states of $TCNQ^-$ in Fig. 8 (a). This interpretation is reasonable since the interchain coupling between neighboring TTF and TCNQ stacks requires the half-filled orbitals of TTF^+ and $TCNQ^-$ to lie in the same region near E_F.[34] Also, magnetic studies[39] of TTF-TCNQ suggest that at room temperature the electrons of the TTF stacks are more delocalized than those on the TCNQ stacks, which support a model with TTF^+ states lying near E_F.

The other relatively weak extrema in Fig. 8 (c), at -1.6 and -2.1 eV, arise primarily from the position mismatch (several tenths of an eV) of the peaks near -2 eV in Figs. 8 (a) and 8 (b). This mismatch is probably due to a sensitivity of this orbital's energy to the interactions between neighboring TCNQ sites in the molecular stack. The TCNQ $3b_{1u}$ orbital is known from recent *ab initio* calculations to be highly delocalized,[36] and the neighbor configuration in $Cs_2(TCNQ)_3$ is very different from that in TTF-TCNQ.[17,28] In addition, influences by neighbor molecules on the orbital energies will be more prevalent in these charge transfer crystals than in simple molecular solids because the partially ionic character of the bonding gives rise to longer-range intermolecular interactions.

The strong excess emission at -2.8 eV in Fig. 8 (c) is assigned to TTF^+ states. This peak cannot be attributed to TTF^0 states since TTF^0 would also give rise to a strong emission peak at about 2 eV higher energy, near -1 eV (see Fig. 14 and Refs. 10 and 11) whereas there is no evidence of such structure in Fig. 8 (c). On this basis we conclude that TTF^0 is not present near the surface of the sublimed TTF-TCNQ at room temperature.

Assignment of the peaks at -0.5 and -2.8 eV in Fig. 8 (c) to the upper two occupied orbitals of TTF^+ is consistent with our earlier considerations, since upon the conversion $TTF \rightarrow TTF^+$, the orbital readjustment would be expected to increase the energy separation of these two levels. In TTF^0 this separation is roughly 2.0 eV (see Fig. 14) and in TTF^+, our assignment gives a separation of 2.3 eV. The schematic diagram for this orbital level shifting is shown in Fig. 9, along with a comparison between experimental level spacings and those from extended-Hückel and[34,40] multiple-scattering $X\alpha$[35] calculations. As in the case of $TCNQ^-$, the Hückel results are surprisingly accurate for the level spacing in TTF^+. Also, the results compare more favorably with experiment when the mixing between empty d orbitals and occupied orbitals is neglected, which confirms the speculation by Berlinsky *et al.*[34] (based on the positions of virtual orbitals in their calculation)

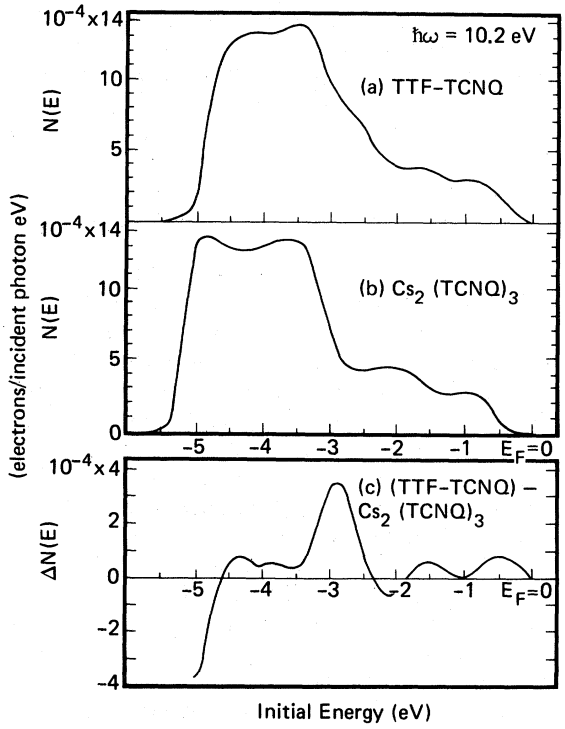

FIG. 8. Comparison of EDC for $\hbar\omega = 10.2$ eV between TTF-TCNQ and $Cs_2(TCNQ)_3$. (a) TTF-TCNQ, (b) Cs_2-$(TCNQ)_3$, (c) difference curve.

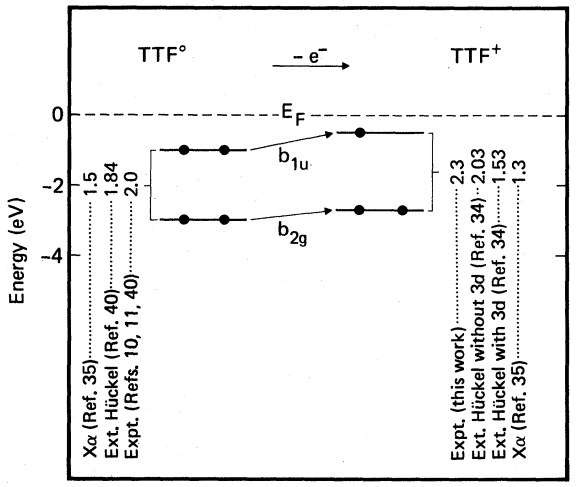

FIG. 9. Schematic diagram of orbital rearrangement in TTF due to electron transfer and comparison of level spacings with recent calculations. Levels are referred to E_F rather than to vacuum since the TTF^0 and TTF^+ results are derived from different experiments with different vacuum levels.

that such mixing is not important. We note that all the recent calculations of TTF^0 and TTF^+ are in agreement with respect to their symmetry assignments of the highest- and second-highest-occupied orbitals to the $4b_{1u}$ and $3b_{2g}$ states, respectively.

D. Surface composition of TTF-TCNQ films

As noted earlier, the UPS spectra of TTF-TCNQ films depend strongly on the substrate temperature at deposition and on the sample's subsequent thermal history. Figures 10 and 11 show the EDC's from TTF-TCNQ films formed and measured on substrates kept at room temperature and liquid-nitrogen temperature, respectively. The four pieces of structure nearest to E_F in Fig. 10 remain stationary in initial energy as photon energy is varied, and the intensities of these structures show relatively little modulation with $\hbar\omega$ after they are completely uncovered from the threshold. These structures are assigned to structures in the valence density of states at -0.9, -1.7, -2.8, and -3.6 eV, respectively. The lower-lying structure below -4 eV moves with respect to the initial energy as $\hbar\omega$ changes. It most likely corresponds to strong density-of-states structure peaked near -7 eV, as reported by Grobman *et al.*[10] with $\hbar\omega = 21.2$ eV, and thus in the present data is not completely cleared of the threshold function. Differences between the EDC's in Fig. 11 and those in Fig. 10 are evident. Not only do the structure positions differ (for the LNT data they lie at -1.1, -2.0, -3.0, -4.3 and below -6.4 eV, respectively), but also the relative intensities of structures are quite different.

As the temperature of the LNT film was slowly increased, the EDC's went through several changes and stabilized to the RT spectra once the temperature had reached about $+8$ °C. This behavior is illustrated for $\hbar\omega = 10.2$ eV in Fig. 12. From -193 to about -80 °C there are essentially no changes. Near -80 °C the first major changes occur. From -78 to -24 °C the EDC's again remain virtually unchanged except for a slight sharpening of structure. Above -24 °C the second major changes set in and the EDC's stabilize to the RT form above $+8$ °C. Upon recooling the sample to -193 °C after it had been warmed to different temperatures, it was found that all the changes observed at any stage of the warming process were irreversible. Furthermore, deposition of TTF-TCNQ on substrates held at any intermediate temperature reproduced the EDC's of an LNT film warmed to that temperature. The irreversibility of the observed changes was confirmed by cooling samples deposited at RT to LNT (Fig. 13). These experiments showed no significant temperature dependence of the EDC's.

In light of the short electron escape depth, the mechanism that causes the changes of the UPS spectra must have altered the electronic states near the surface. We propose here a model through which the observed major changes can be consistently explained: We postulate that during sublimation of the starting TTF-TCNQ material onto an LNT substrate, some percentage of the molecules condensed as uncomplexed neutral species, TTF^0 and $TCNQ^0$, and some condensed as the associated complex TTF-TCNQ, thereby forming a mixed solid having UPS spectra which are to a first approximation weighted sums of the spectra of the three components. As the sample temperature was increased above -80 °C, molecular reorientations and rearrangements could take place to minimize the potential energy of the system.

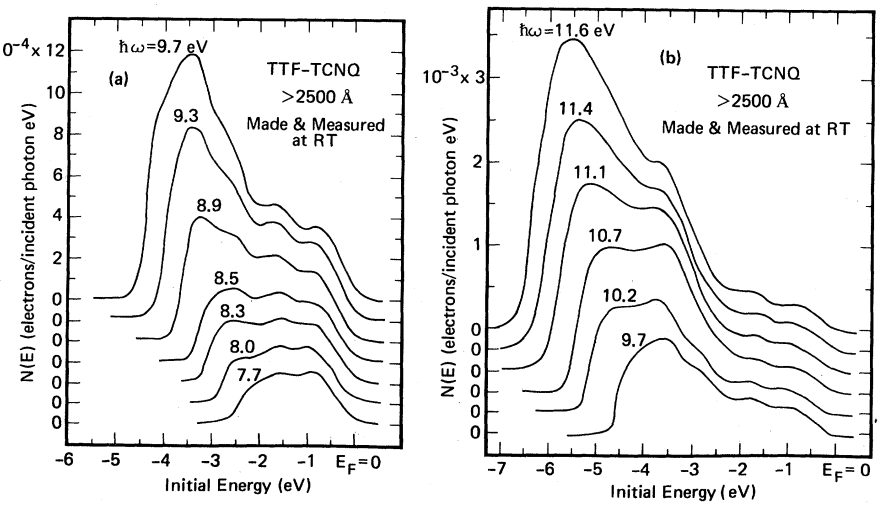

FIG. 10. EDC's from an RT-made-and-measured TTF-TCNQ film. (a) $7.7 \leq \hbar\omega \leq 9.7$ eV, (b) $9.7 \leq \hbar\omega \leq 11.6$ eV. Ordinate scale is different from (a).

This favored a configuration in which the component molecules with highest vapor pressure, i.e., TTF^0, populate the surface.[41] This in turn made emission from TTF^0 most prominent in the UPS spectra in the temperature range from −80 to −24 °C. As temperature was increased further, TTF^0 escaped from the surface because of its high vapor pressure and the RT spectra became dominated by emissions from TTF-TCNQ and $TCNQ^0$.

In addition to the irreversibility of the changes in the EDC's, and the conclusion arrived at in Sec. III C that TTF^0 is not present at the surface of a sublimed TTF-TCNQ film at RT, there are several other experimental facts consistent with the above model. The first evidence is the growth of the peak near −1 eV in the UPS spectra, which is characteristic of TTF^0,[10,11] as the temperature increases from LNT to −24 °C. This is shown in Fig. 14, where we compare EDC's of LNT-formed TTF-TCNQ to that of TTF^0 taken by Nielsen *et al.*[42] The important points here are that the peak in the vicinity of −1 eV grows by about a factor of 2 as the temperature is increased and that the relative peak and valley positions of the −24 °C data match quite well with the TTF^0 spectrum. Also note that in Fig. 14 the TTF^0 EDC has a threshold energy about 1 eV below that of the other two curves, which allows the uncovering of the strong peak at about −5.0 eV. Since the photoemission threshold can be very sensitive to the way the films are prepared, the difference between the TTF^0 data and our −24 °C TTF-TCNQ data in the low-energy region is not surprising. The greater emission intensities below −2.5 eV for TTF^0 may be due in large part to this lower threshold energy.

If the proposed model is correct in explaining the observed changes in EDC's, we would expect that a weighted sum of UPS spectra which combines data from an LNT TTF-TCNQ film warmed to 24 °C (i.e., mostly representing TTF^0 at the surface) and from an RT film (i.e., representing $TCNQ^0$ and TTF-TCNQ) would approximately reproduce the spectrum of an as-deposited LNT film. We present the result of this analysis in Fig. 15, where the weighted composite spectrum and the LNT spectrum are compared.[43] The two curves in Fig. 15 agree with each other in salient features except for the region near the trailing edge (left-hand side) and slight differences between E_F and −2.0 eV. The smaller photoemission threshold for the LNT film than for the RT or −24 °C data (more than 0.2 eV smaller) is the primary reason for the stronger emission intensity below −4 eV in the LNT EDC. The reason for the small discrepancies between E_F and −2.0 eV will become clearer from the discussions in Sec. III E. Despite these minor differences, the agreement between the two curves in Fig. 15 is sufficiently good to support the applicability of our model.

Further evidence in support of the above-mentioned model comes from the data of differential

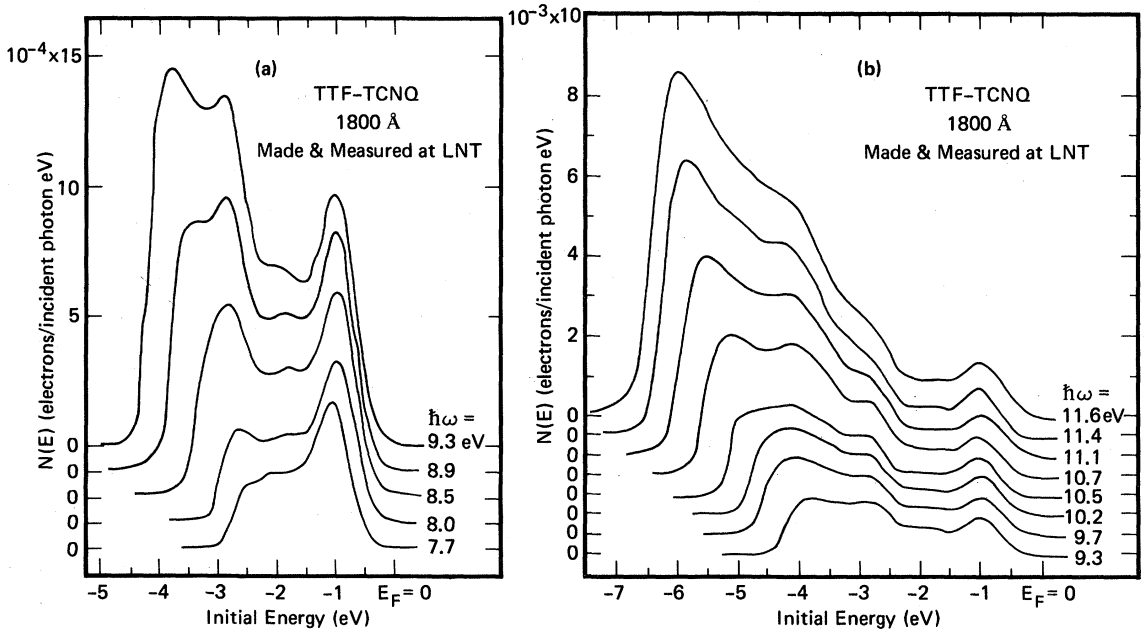

FIG. 11. EDC's from an LNT-made-and-measured TTF-TCNQ film. (a) $7.7 \leq \hbar\omega \leq 9.3$ eV, (b) $9.3 \leq \hbar\omega \leq 11.6$ eV. Ordinate scale is different from (a).

thermal analysis (DTA), which measures the heat capacity of the sample relative to a reference (He gas in this case) during warming at a constant rate. The DTA data were taken from TTF-TCNQ condensed onto substrates kept at LNT and then warmed for the first time during the thermal analysis run. In Fig. 16 (a) the temperature difference ΔT between the sample and the reference is plotted as a function of the sample temperature during its initial warming from LNT. In Fig. 16 (b) the same sample was cooled back down to LNT and remeasured during a second warming.

Figure 16 (a) shows a monotonic decrease in ΔT superimposed with two broad peaks in the range between -50 and -15 °C plus a sharp negative spike near 0 °C. In Fig. 16 (b) the two broad peaks are missing. The repeatable downward spike near 0 °C is attributed to the endothermic melting of ice, which probably accumulated on the sample during the 3 sec period in which it was exposed to air upon transfer from the sublimation chamber to the DTA apparatus. On the other hand,

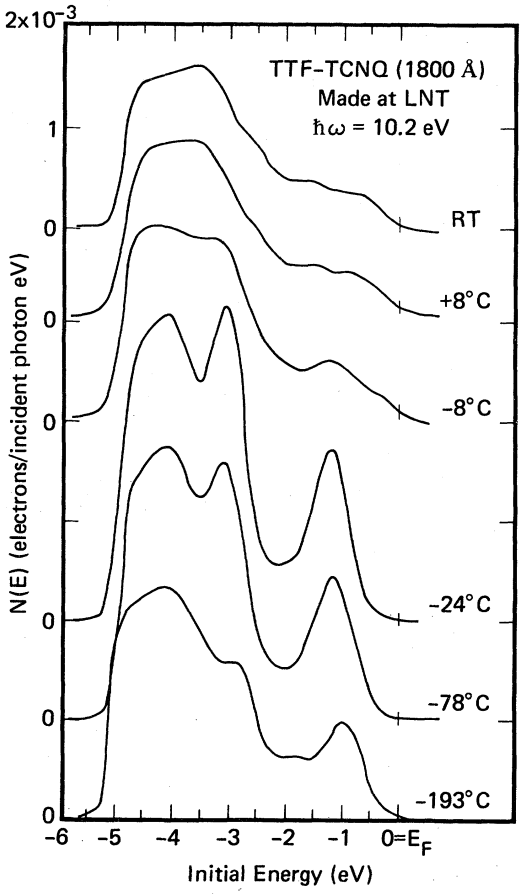

FIG. 12. EDC's for $\hbar\omega = 10.2$ eV from an LNT-made TTF-TCNQ film as measurement temperature is increased.

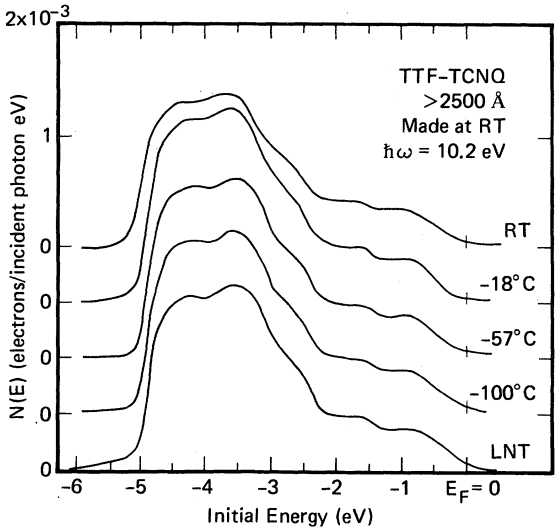

FIG. 13. EDC's for $\hbar\omega = 10.2$ eV from an RT-made TTF-TCNQ film cooled to different temperatures.

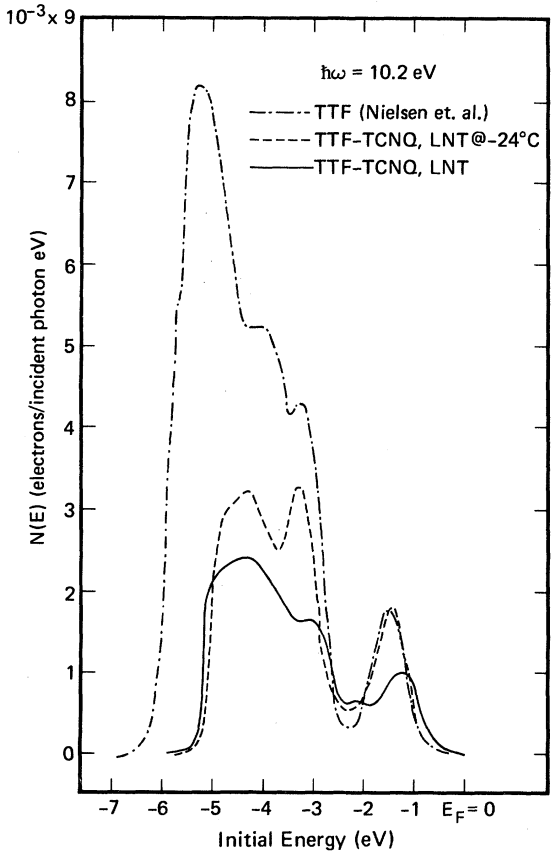

FIG. 14. Comparison of EDC's from an LNT-made TTF-TCNQ film at different temperatures to that from TTF^0 (Ref. 42). Absolute emission intensities are not available for the TTF^0 spectrum, which has been normalized to make the leading peak the same peak height as that of the −24 °C TTF-TCNQ spectrum.

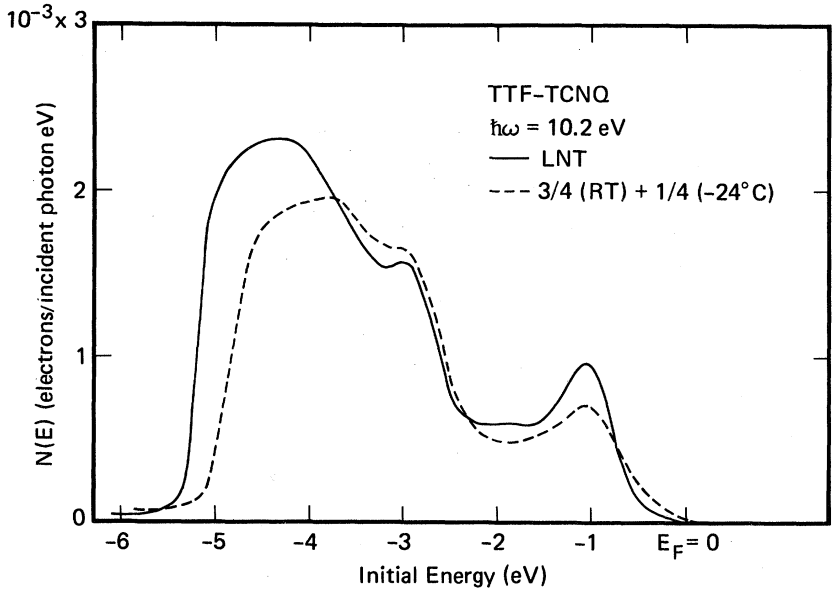

FIG. 15. EDC's for $\hbar\omega$ =10.2 eV from an LNT-made TTF-TCNQ film. Solid curve was measured at LNT; broken curve calculated using a weighted sum of curves measured at RT and −24 °C.

the two nonrepeatable peaks manifest two bulk transitions in the TTF-TCNQ solid.

The DTA data are consistent with our model in important aspects. The occurrence of the two peaks between LNT and RT indicates that molecular rearrangements and reorientations occur between these two temperatures. The fact that the peaks disappeared in the second run attests to the irreversibility of these changes upon warming to RT. These facts are in good agreement with our observations in photoemission data and are consistent with our model. Furthermore, although our UPS spectra are surface sensitive while the DTA results are indicative of changes throughout the bulk solid, it is plausible that the thermally induced molecular rearrangements in the bulk facilitate the movement of TTF^0 to the sample surface.

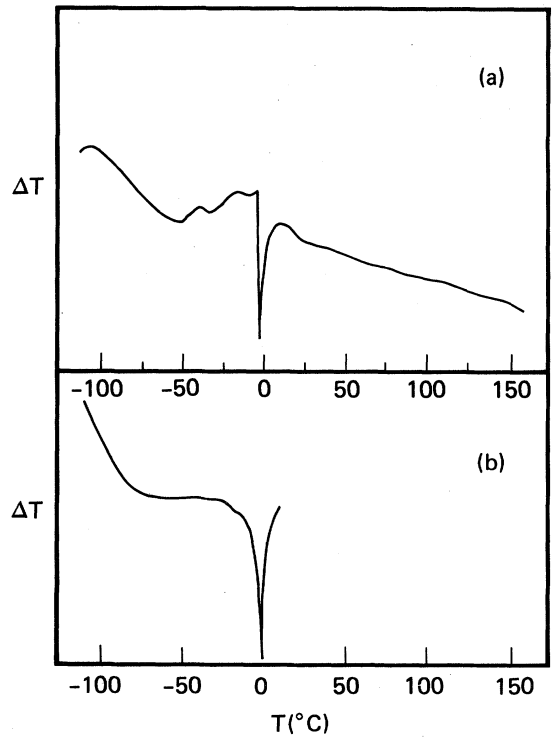

FIG. 16. Differential thermal analysis of LNT-made TTF-TCNQ. ΔT were measured using He gas as the reference. (a) LNT-made sample warmed to 150 °C; (b) After (a), sample was recooled to LNT, and then warmed to above 0 °C during the measurement.

One point of concern is that the two peaks in the DTA spectra do not appear at the same temperatures where the UPS spectra were observed to change (between −50 and −15 °C for DTA and at about −78 °C and from −24 to +8 °C for UPS). This discrepancy may be attributed to the greatly different heating rates employed in the two experiments. In the photoemission experiment, the temperature range from LNT to RT was spanned in about 24 h, and no attempt was made to hold the warming rate constant, it being greater at lower temperature. In the DTA experiment, on the other hand, the warming rate was held constant at 10 °C/min. Had it been possible to set constant and equal warming rates in both cases, the transitions would probably have been observed at closer temperatures in the two experiments.

E. Long-range order and charge transfer in TTF-TCNQ

A final point to consider involves the changes in the EDC's of TTF-TCNQ just below room temperature, especially in the region between E_F and

−2.0 eV. In our RT data, this region contains the two-peaked structure shown to be characteristic of $TCNQ^-$ anions. In the LNT-deposited films these peaks do not begin to appear until the temperature has increased above −8 °C. Furthermore, the high-temperature EDC's exhibit considerable electron emission intensity in the immediate vicinity below E_F that is absent in all the curves below −8 °C in Fig. 12. In the context of the model proposed above, most of the changes in this energy range must be associated with changes in the electronic structure of the TTF-TCNQ complex pairs, since we have argued that TTF° is no longer present at the surface near room temperature, and $TCNQ^\circ$ does not contribute to the electron emission above −2.5 eV.

The fact that the two-peaked structure appeared gradually only after the LNT-deposited TTF-TCNQ films were annealed above −8 °C suggests that the associated TTF-TCNQ pairs which condensed onto the substrates held at LNT are somewhow different in character from the TTF-TCNQ pairs in the RT films. This view is strengthened by the fact that no irreversible changes or annealing effects were seen in the electronic structure when we conducted the warming UPS experiments on LNT-deposited films of $TCNQ^0$. The difference can be understood in the following terms: Because the energy required to transfer charge in TTF-TCNQ is relatively large[44] (>1 eV in the solid), compensation by the complete Madelung energy of an ordered ionic lattice is required to allow a stable ground state in which one electron has been transferred from each TTF to a TCNQ. At LNT the TTF-TCNQ films as deposited may be highly disordered such that the associated pairs of TTF-TCNQ involve only slight charge transfer. Upon warming, increasing amounts of long-range order set in[45] and the Madelung contribution to the lattice energy stabilizes the ionized system.

It has been established[46] for low-temperature-deposited films of alkali halides and thallous halides that the more polarizable the deposited species, the higher the temperature at which one must anneal the films to bring about long-range order, since the stabilizing electrostatic forces of the ordered lattice are more heavily screened. The most polarizable system studied in the halide work was TlI, which required annealing at 140 °K to restore long-range order. In the present case the TTF and TCNQ molecules are more polarizable than Tl and I; hence our films must be warmed to higher temperature (at least −8 °C) to stabilize the crystal structure.

IV. CONCLUSIONS

In conclusion, photoemission has been used to investigate the electronic structure of *in-situ*-formed thin films of TTF-TCNQ, TCNQ, and $Cs_2(TCNQ)_3$. The electron escape depth in TTF-TCNQ has been estimated to be less than 10 Å, and it has been suggested that this short escape depth may be a general property of many TCNQ-based compounds as well as other organic solids. Thus UPS spectra of these solids have been interpreted as containing a strong representation of the surface electronic structure of the samples.

Five maxima in the EDC's of room-temperature TTF-TCNQ films have been associated with maxima in the valence density of states. Through comparison to EDC's of $Cs_2(TCNQ)_3$, the origins of these maxima have been assigned. Summaries of these results and a comparison with those of Ref. 10 are presented in Table I.

Table I confirms the existence of $TCNQ^0$ in room-temperature TTF-TCNQ while it argues against the presence of TTF^0. This suggests that whereas TTF^0 may be captured in low-temperature-deposited films of TTF-TCNQ, little of this species remains at the surface of a room-temperature TTF-TCNQ film. Table I also indicates a TTF^+

TABLE I. Origins of UPS structures of TTF-TCNQ films.

Reference 10		Present studies	
Structure position with respect to E_f (eV)	Origin	Origin	Structure position with respect to E_f (eV)
		TTF^+ $(4b_{1u})$ [a]	−0.5
−1.0	$TCNQ^-$, TTF^0, TTF^+	$TCNQ^-$ $(3b_{2g})$ [b]	−0.9
−1.9	$TCNQ^-$	$TCNQ^-$ $(3b_{1u})$ [b]	−1.7
−3.0	TTF^0, TTF^+	TTF^+ $(3b_{2g})$ [a]	−2.8
−4.1	$TCNQ^-$	$TCNQ^0$ $(3b_{1u})$ [b] $TCNQ^-$	−3.6

[a] Symmetry assignments from Refs. 34 and 35.
[b] Symmetry assignments from Refs. 35–37.

level slightly below E_F. This assignment is consistent with the two-band description of TTF-TCNQ arising from parallel cation and anion stacks.

Strong dependence of UPS spectra of TTF-TCNQ on substrate temperature at deposition and its subsequent thermal history has been found. An explanation of this effect has been offered in terms of a change in the surface composition with temperature and an increased degree of ionization of TTF-TCNQ pairs accompanying disorder-to-order transitions. More specifically, the surface region of the samples consists of TTF^0, $TCNQ^0$, and only-slightly-ionized TTF-TCNQ pairs at LNT, is dominated by TTF^0 from -80 to -24 °C and is composed of neutral $TCNQ^0$ and ionized TTF-TCNQ at room temperature. This explanation is not only consistent with the short escape depth and the disappearance of TTF^0 at the sample surface at RT, but also in good agreement with the details of the UPS spectra of samples of different thermal history. It has further been shown to be consistent with the results of differential thermal analysis. The peak positions of UPS spectra of LNT TTF-TCNQ films annealed to the temperature range from -80 to -24 °C are summarized in Table II in comparison to data from TTF^0 taken by Nielsen *et al.*[11] The degree of ionization between TTF and TCNQ in TTF-TCNQ pairs, suggested to be different in the disordered LNT state and the polycrystalline RT state, has been rationalized in terms of the long-range Madelung contribution to the energy needed for the stabilization of the ionized system.

Several experiments suggest themselves to provide a definitive test of this model. Auger electron spectroscopy studies performed on *in-situ*-prepared LNT TTF-TCNQ films would in principle allow one to monitor the surface concentration of sulphur atoms (in TTF) as a function of substrate temperature. Thus it may be possible to see the change of surface composition as LNT films are warmed. This experiment is expected to be difficult since preliminary electron impact experiments[47] indicate that these solids suffer radiation damage readily. Equally useful experiments to test the validity of the proposed model include ultrahigh-vacuum mass spectroscopy and *in situ* x-ray diffraction. The former measurement could examine whether TTF^0 vapor species are released from the films at -24 °C, and the latter could ascertain whether the proposed changes in long-range order take place at the transition temperatures.

The EDC's of TTF-TCNQ at all temperatures (Figs. 10–12) show very little electron population at E_F. This result is in contrast to the metallic electrical behavior of TTF-TCNQ, and must be attributed, as discussed by others,[10,11] to localization of the states in question, at least for time scales of $\sim 10^{-16}$ sec. It has previously been suggested that this localization is primarily attributable to strong electron-phonon coupling in this system.[10,11] However, since the electron escape depth for UPS studies has been shown to be unusually small, the localized nature of the electronic states near E_F may be equally attributable to the influence of the surface.

The coexistence of $TCNQ^0$ and $TCNQ^-$ in TTF-TCNQ has been confirmed in the present studies, in agreement with the conclusions of previous authors.[10] However, the coexistence may occur only in the surface region of the samples. We cannot rule out the possibility that $TCNQ^0$ resides mostly near the surface since there the complete Madelung stabilization energy is not available to enhance charge transfer. Recent high-resolution XPS studies[48] of the N(1s) levels in TTF-TCNQ suggest that the concentration of $TCNQ^0$ is highly sensitive to the surface preparation of the sample, which argues for the existence of $TCNQ^0$ primarily at the surface.

In $Cs_2(TCNQ)_3$, it is clear that both $TCNQ^0$ and $TCNQ^-$ can reside in the bulk as well as at the surface, since stoichiometry requires the presence of $TCNQ^0$ in the bulk and the lower charge transfer energy (about 3 eV less than in TTF-TCNQ) allows the presence of $TCNQ^-$ at the surface. In TTF-TCNQ, on the other hand, the situation is less clear. Until this issue can be more definitively resolved, the exact degree of charge transfer cannot be quantitatively determined by these types of experiments. However, to the extent that it is fair to generalize from the results of the Cs-TCNQ system, our data suggest that if partial charge transfer does occur in the bulk of TCNQ salts, it will probably take the form of a mixture of neutrals and ions, rather than a homogeneous arrangement of fractionally ionized molecules.

ACKNOWLEDGMENTS

The authors are indebted to G. Castro, U.T. Mueller-Westerhoff, and R. Schumaker for pro-

TABLE II. Comparison of UPS peak positions at $\hbar\omega = 10.2$ eV.

LNT TTF-TCNQ (−80 to −24 °C) (eV)	TTF^0 from Ref. 11 (eV)
−1.3	−1.3
−3.3	−3.3
−4.3	−4.0

viding TCNQ and TTF-TCNQ materials in a highly purified form. They are also grateful to G.B. Street for his help in the DTA measurements and P. Nielsen for providing his unpublished TTF^0 data and stimulating discussions. They wish to express their appreciation to P. McKernan, S. Werner, and F. Peters of the Stanford Tube Laboratory for their technical contributions, and to thank W.D. Grobman, J.A. Hertz, and many colleagues at Stanford and IBM for helpful interactions.

---

[1]J. P. Ferraris, D. O. Cowan, V. V. Walatka, and J. H. Perlstein, J. Am. Chem. Soc. 95, 948 (1973).
[2]L. B. Coleman, M. J. Cohen, D. J. Sandman, F. G. Yamagishi, A. F. Garito, and A. J. Heeger, Solid State Commun. 12, 1125 (1973).
[3]A. N. Bloch, J. P. Ferraris, D. O. Cowan, and T. O. Poehler, Solid State Commun. 13, 753 (1973).
[4]P. M. Grant, R. L. Greene, G. C. Wrighton, and G. Castro, Phys. Rev. Lett. 31, 1311 (1973).
[5]C. W. Chu, J. M. E. Harper, T. H. Geballe, and R. L. Greene, Phys. Rev. Lett. 31, 1491 (1973).
[6]J. Bardeen, Solid State Commun. 13, 357 (1973); D. Allende, J. W. Bray, and J. Bardeen, Phys. Rev. B 9, 119 (1974).
[7]P. A. Lee, T. M. Rice, and P. W. Anderson, Phys. Rev. Lett. 31, 462 (1973).
[8]B. R. Patton and L. J. Sham, Phys. Rev. Lett. 31, 631 (1973).
[9]R. P. Groff, A. Suna, and R. E. Merrifield, Phys. Rev. Lett. 33, 418 (1974).
[10]W. D. Grobman, R. A. Pollack, D. E. Eastman, E. T. Mass, Jr., and B. A. Scott, Phys. Rev. Lett. 32, 534 (1974).
[11]P. Nielsen, A. J. Epstein, and D. J. Sandman, Solid State Commun. 15, 53 (1974).
[12]W. E. Spicer and C. N. Berglund, Rev. Sci. Instrum. 35, 1665 (1964); R. C. Eden, *ibid.* 41, 252 (1970).
[13]R. S. Bauer, Ph.D. dissertation (Stanford University, 1970) (unpublished).
[14]T. H. Chen and B. H. Schechtman, Bull. Am. Phys. Soc. 18, 1597 (1974); T. H. Chen and B. H. Schechtman, Thin Solid Films 30, 169 (1975).
[15]T. H. DiStefano, Ph.D. dissertation (Stanford University, 1970) (unpublished).
[16]We assume that the deposition rate is independent of the sample thickness.
[17]C. J. Fritchie and P. Arthur, Acta Crystallogr. 21, 139 (1966).
[18]W. J. Siemons, P. E. Bierstedt, and R. G. Kepler, J. Chem. Phys. 39, 3523 (1963).
[19]E. T. Mass, Jr., Mater. Res. Bull. 11, 873 (1974).
[20]N. Uyeda, T. Kobayashi, and E. Suito, in *Proceedings of the Seventh International Congress on Electron Microscopy*, Vol. II, edited by P. Favard (French Society of Electron Microscopy, Paris, 1970).
[21]I. Lindau and W. E. Spicer, J. Electron. Spectrosc. Related Phenomena 3, 409 (1974).
[22]J. L. Shay and W. E. Spicer, Phys. Rev. 161, 799 (1967).
[23]Equation (2) takes into account only electrons emitted from the film, since Fig. 1 and Fig. 2 showed no evidence of electrons emitted from the gold substrate.
[24]A consideration of optical sum rules indicates that values of α higher than a few times 10^6 cm^{-1} are unrealistic in the vacuum uv region for TTF-TCNQ.
[25]P. W. Palmberg and T. N. Rhodin, J. Appl. Phys. 39, 2425 (1968).
[26]G. Castro (unpublished).
[27]R. E. Long, R. A. Sparks, and K. N. Trueblood, Acta Crystallogr. 18, 932 (1965).
[28]T. E. Philips, T. J. Kistenmacher, J. P. Ferraris, and D. O. Cowan, Chem. Commun. 14, 471 (1973).
[29]P. Chaudhari, B. A. Scott, P. B. Laibowitz, Y. Tomkiewicz, and J. B. Torrance, Appl. Phys. Lett. 24, 439 (1974).
[30]P. M. Chaikin, J. F. Kwak, T. E. Jones, A. F. Garito, and A. J. Heeger, Phys. Rev. Lett. 31, 601 (1973).
[31]F. J. Piepenbring, *Optical Properties and Electronic Structure of Metals and Alloys*, edited by F. Abelés (North-Holland, Amsterdam, 1966).
[32]W. Pong and J. A. Smith, J. Appl. Phys. 44, 174 (1973).
[33]B. H. Schechtman, S. F. Lin and W. E. Spicer, Phys. Rev. Lett. 34, 667 (1975).
[34]A. J. Berlinsky, J. F. Carolan, and L. Weiler, Solid State Commun. 15, 795 (1974); and unpublished.
[35]I. P. Batra, B. I. Bennett and F. Herman, Phys. Rev. B 11, 4927 (1975).
[36]H. Johansen, Theor. Chim. Acta (to be published).
[37]H. T. Jonkman, G. A. van der Velde, and W. C. Niewpoort, Chem. Phys. Lett. 25, 62 (1974).
[38]C. E. Klots, R. N. Compton, and V. F. Raaen, J. Chem. Phys. 60, 1177 (1974).
[39]Y. Tomkiewicz, B. A. Scott, L. J. Tao, and R. S. Title, Phys. Rev. Lett. 32, 1363 (1974).
[40]R. Gleiter, E. Schmidt, D. O. Cowan, and J. P. Ferraris, J. Electron. Spectrosc. Related Phenomena 2, 207 (1973).
[41]Bonds involving molecules of higher vapor pressure correspond to higher potential energy. An arrangement with these molecules populating the surface minimizes the number of these bonds and thereby minimizes the potential energy of the system. See F. L. Williams, Ph.D. dissertation (Stanford University, 1972) (unpublished).
[42]P. Nielsen (private communication).
[43]The −24 °C data have been shifted upward by 0.2 eV and the relative weighting of the composite curve's components has been selected to produce the best agreement with the LNT data.
[44]The exact amount of charge transfer in the solid is determined by a delicate balance of the molecular charge transfer energy, polarizability of both electron donor and acceptor and the long-range electrostatic Madelung energy. We use a charge transfer energy in the solids defined as ionization potential of electron donor minus electron affinity of electron acceptor and minus dielectric relaxation energy of the lattice. We have an ionization energy of TTF of 6.8 eV (Ref. 40), and an electron affinity of TCNQ of 2.8 eV (Ref. 38), and assume a typical polarization energy of an elec-

tron-hole pair in molecular solids of ~3 eV.
[45]Structural studies (Ref. 14) of LNT TTF-TCNQ films warmed to RT indicate that the films possess the same crystal structure as bulk solution-grown crystals.
[46]R. Hilsch, in *Non-Crystalline Solids*, edited by V. D. Fréchette (Wiley, New York, 1960).
[47]H. F. Winters (private communication).
[48]B. H. Schechtman, S. F. Lin, and W. E. Spicer (unpublished).